

PAPER • OPEN ACCESS

## Effect of pressure on optical properties of the transition metal dichalcogenide $\text{MoSe}_2$

To cite this article: S Caramazza *et al* 2017 *J. Phys.: Conf. Ser.* **950** 042012

View the [article online](#) for updates and enhancements.

### You may also like

- [Evaluation of Strain-Shift Coefficients for SiSn by Raman Spectroscopy](#)  
Ryo Yokogawa, Masashi Kurosawa and Atsushi Ogura
- [In Situ Raman Diagnostics of Intercalation Batteries](#)  
Christian Hess and Toni Gross
- [Electrochemical in-Situ Raman Spectroscopic Studies of Highly-Cycled Li\(Ni/Co/Mn\)O<sub>2</sub> Cathode Cells](#)  
Tadashi Awatani, Ritsuko Kitano, Teruhisa Baba *et al.*

### Recent citations

- [Mn-intercalated MoSe<sub>2</sub> under pressure: Electronic structure and vibrational characterization of a dilute magnetic semiconductor](#)  
Shunda Chen *et al*
- [Structural Phase Transition and Bandgap Control through Mechanical Deformation in Layered Semiconductors 1T-ZrX<sub>2</sub> \(X = S, Se\)](#)  
Edoardo Martino *et al*
- [High pressure anomalies in exfoliated MoSe<sub>2</sub>: resonance Raman and x-ray diffraction studies](#)  
Pinku Saha *et al*



The Electrochemical Society  
Advancing solid state & electrochemical science & technology

## 241st ECS Meeting

May 29 – June 2, 2022 Vancouver • BC • Canada

Extended abstract submission deadline: Dec 17, 2021

Connect. Engage. Champion. Empower. Accelerate.  
Move science forward



Submit your abstract



# Effect of pressure on optical properties of the transition metal dichalcogenide MoSe<sub>2</sub>

S Caramazza<sup>1</sup>, F Capitani<sup>1,2</sup>, C Marini<sup>3</sup>, A Mancini<sup>4</sup>, L Malavasi<sup>4</sup>, P Dore<sup>5</sup> and P Postorino<sup>1</sup>

<sup>1</sup> Dipartimento di Fisica, Università di Roma Sapienza, Piazzale Aldo Moro 2, 00185 Roma, Italy

<sup>2</sup> Synchrotron SOLEIL, L'Orme des Merisiers Saint-Aubin, BP 48, F-91192 Gif-sur-Yvette Cédex, France

<sup>3</sup> CELLS-ALBA, Carretera - BP 1413, Cerdanyola del Vallés, 08290, Barcellona, Spain, EU

<sup>4</sup> Dipartimento di Chimica, Università di Pavia, Via Taramelli 16, 27100 Pavia, Italy

<sup>5</sup> CNR-SPIN and Dipartimento di Fisica, Università di Roma Sapienza, P.le Aldo Moro 2, 00185 Roma, Italy

E-mail: paolo.postorino@roma1.infn.it

**Abstract.** Transition Metal Dichalcogenides TMDs MoX<sub>2</sub> (X=S, Se, Te) are an emergent class of layered materials displaying exciting optoelectronic properties which can be modified by varying the number of layers, by intercalation, or by applying an external strain/compression. In particular, these semiconducting materials can get a band gap closure under pressure and enter in a metallic phase. Here, we investigate the optical properties of MoSe<sub>2</sub> under high pressure by means of Raman spectroscopy over a wide pressure range (0-30 GPa). No anomaly has been observed in the pressure dependence of the frequencies of the vibrational modes  $A_{1g}$ ,  $E'_{2g}$  (Raman first order) and  $E''_{2g}$  (Raman second-order), in agreement with the absence previously reported of any pressure induced structural transition. Interestingly, our detailed line-shape analysis show a clear anomaly in the pressure behavior of the linewidth of the  $A_{1g}$  and  $E'_{2g}$  phonons at the insurgent metallization process which was observed in previous infrared and transport experiments. Our results indicate that the linewidths of Raman phonons peaks can be sensitive to even subtle pressure-induced electronic rearrangements and can thus be used to monitor the insurgence of a pressure-induced semiconductor-metal transition.

## 1. Introduction

Graphene-like two-dimensional (2D) materials such as layered Transition Metal Dichalcogenides (TMD) attract a lot of interest because of their extraordinary physical and chemical properties, tunable in particular by varying number of layers, thermodynamic conditions (P,T) and doping [1]. Semiconducting TMDs belonging to the family of the MoX<sub>2</sub> compounds (X=S, Se, Te) are layered materials built up of a stacking of X-Mo-X layers [2], consisting of three hexagonal planes, two made by X atoms and one of Mo atoms in between. Within this three-layers structure, Mo is coordinated through covalent interactions with the X atoms in a trigonal prismatic arrangement (symmetry group:  $P6_3/mmc$ ). The distance among the X-Mo-X layers, which is controlled by weak Van Der Waals (VdW) interactions, has a key role in determining the electronic properties of TMDs, such as semiconducting gap and transport properties [2]. Specifically, by strongly reducing the number of



layers and thus the interlayer coupling, the optoelectronic properties of TMDs are significantly changed [1]. For example, in the MoSe<sub>2</sub> case, the bandgap (close to 1.1 eV) is indirect in the bulk system [3], while, in the single layer case, it becomes direct and shifts into the visible range (near to 1.55 eV). This is of great interest since optical properties of MoSe<sub>2</sub> can then be exploited for several potential applications in the visible range (solar cells, photodetectors and so on) [1,3].

In studying the structural and optical properties of TMDs, the high pressure technique is an alternative tool to modify the interlayer distances and thus the interlayer VdW coupling [4]. Indeed, by increasing pressure, TMD semiconducting gap and transport properties can be remarkably modified and, at very high pressure, a semiconducting-metal transition can occur. Recently, x-ray diffraction (XRD) measurements have shown that the MoS<sub>2</sub> system undergoes a subtle isostructural transformation at about 20 GPa (*layer sliding* transformation) with a collapse of the *c*-lattice parameter [5,6,7], in agreement with theoretical computations [8]. Experiments [6] and theoretical calculations [8] also show that the system enters a metallic phase within the same pressure range (19 GPa in ref. [6] and 20-25 GPa in ref. [8]). For MoTe<sub>2</sub>, no x-ray diffraction (XRD) data are available at high pressures, but theoretical calculations show that this system apparently preserves its structure at least up to 100 GPa, and that a complete metallization occurs in the 13-19 GPa pressure range [9].

In the case of MoSe<sub>2</sub>, Aksoy *et al.* [10] carried out XRD measurements up to 36 GPa and do not report any structural transition. More recently, experimental results obtained by Z. Zhao *et al.* [11] seem to confirm that MoSe<sub>2</sub> do not undergoes any structural transformation up to 60 GPa. In studying electronic and transport properties, the same authors also carried out infrared measurements, showing that, in MoSe<sub>2</sub> single crystals, remarkable changes occur with increasing pressure. In particular, they found the onset of a metallization process between 16 and 20 GPa, and within the 20-35 GPa range the energy gap rapidly decreases down to vanishingly small values. Transport measurements performed up to 42 GPa reveal indeed that the metallization process is complete at about 40 GPa [11]. From a theoretical point of view, DFT calculations performed by Rifliková *et al.* [9] predict that MoSe<sub>2</sub> preserves its original structure up to 100 GPa, while it undergoes a complete metallization in the 28-40 GPa pressure range.

In conclusion, pressure dependent XRD structural studies of different MoX<sub>2</sub> systems do not show abrupt or well defined structural transitions, while infrared and transport properties reveal progressive but well detectable pressure-induced transformations in the electronic structure, such as metallization processes. The aim of the present work is to study pressure effects on the optical properties a MoX<sub>2</sub> system by employing Raman spectroscopy, which by probing the phonon spectrum is sensitive to structural properties of the system, but can also probe its electronic state and charge-lattice couplings by a detailed line-shape analysis [6,12,13]. We thus performed Raman measurements on a crystal powder of MoSe<sub>2</sub> in the 0-30 GPa range with the idea of confirming on one side the absence of any structural transition and, on the other side, of carrying out a detailed line-shape analysis looking for a spectroscopic signature of the insurgent metallization process.

## 2. Raman measurements on MoSe<sub>2</sub> at high pressure

The four Raman-active phonons predicted in MoX<sub>2</sub> systems are of  $A_{1g}$ ,  $E_{1g}$ ,  $E_{2g}^1$  and  $E_{2g}^2$  symmetry [2]. The first three modes are due to atomic vibrations within a X-Mo-X layer.  $A_{1g}$  is an out-of-plane mode (where the X atoms move outside the layer, along the *c*-axis). Note that the  $E_{1g}$  and the  $E_{2g}^1$  are in-plane modes: in the former, the X-atoms moves in opposite directions and the Mo-atoms do not move at all; in the latter, the X-atoms of adjacent layers move in opposite direction. The fourth mode,  $E_{2g}^2$ , is called “rigid-mode” and correspond to the relative motion of two adjacent X-Mo-X rigid layers. In the Raman spectrum of a MoSe<sub>2</sub> single crystal, Sekine *et al.* [14] observed the  $E_{2g}^2$  (25.4 cm<sup>-1</sup>)  $A_{1g}$  (242 cm<sup>-1</sup>) and  $E_{2g}^1$  (286 cm<sup>-1</sup>) phonons. For the  $E_{1g}$  mode, they found that it can be detected at 168 cm<sup>-1</sup> only with polarized incident radiation. In the measured spectra, also second-order Raman contributions were observed. In particular, spectral features above 300 cm<sup>-1</sup> were assigned to a two-phonon overtone or combination bands and the peak at 145 cm<sup>-1</sup> to a two-phonon difference process [14], recently ascribed to the  $E_{1g} - E_{2g}^2$  combination band [15].

In the present work, we collected Raman spectra of MoSe<sub>2</sub> crystal powder (Sigma Aldrich: 325 mesh, 99.9%) as a function of pressure. Finely milling the sample, we obtained a powder with a micrometric/sub-micrometric average grain size.

A diamond-anvil cell (DAC), equipped with 400  $\mu\text{m}$  culet II A diamonds, was employed in the 0-30 GPa pressure range. The gasket was made of a 250- $\mu\text{m}$ -thick steel foil, with a sample chamber of 100  $\mu\text{m}$  diameter and 50  $\mu\text{m}$  height. A small quantity of powder of MoSe<sub>2</sub> was loaded inside the gasket hole together with NaCl powder used as hydrostatic medium. A ruby sphere was also put close to the sample into the sample chamber to measure the pressure through the standard ruby fluorescence techniques [16].

Raman measurements were carried out by means of a Horiba LabRAM HR Evolution microspectrometer using a 30 mW He-Ne laser (632.8 nm wavelength). The spectrometer is equipped with a notch filter used to reject the elastic contribution, a grating monochromator, and a Peltier-cooled charge-coupled device (CCD) detector. A confocal microscope with long working distance objectives is used to focus the laser beam on the sample and to collect the scattered signal. For the present measurements we used a 50x objective allowing a few-micrometer diameter laser spot on the sample. Raman spectra were collected in the backscattering geometry over the 120-500  $\text{cm}^{-1}$ , with a spectral resolution better than 1  $\text{cm}^{-1}$  thanks to a 1800 grooves/mm grating with a 800-mm focal length. Further details about the Raman experimental setup can be found in ref. [17].

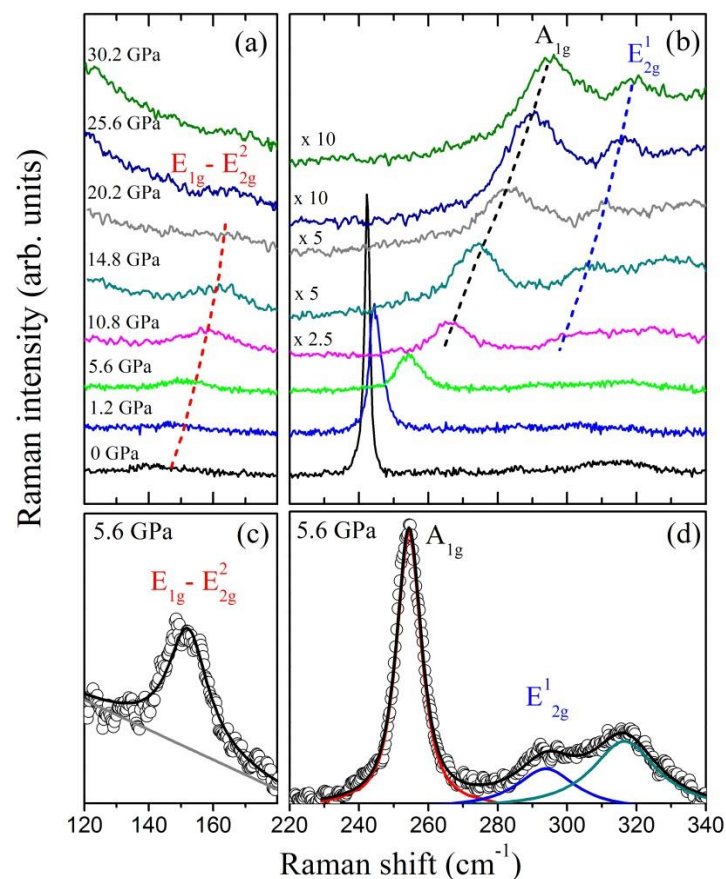


**Figure 1.** (a)-(b) Raman spectra of crystal powder of MoSe<sub>2</sub> as function of pressure at selected pressures. Dashed lines are guides for the eye. (c)-(d) the three vibrational modes ( $A_{1g}$ ,  $E_{2g}^1$  and  $E_{1g} - E_{2g}^2$ ) and best fit profiles are shown for the 5.6 GPa pressure.

The Raman spectra of MoSe<sub>2</sub> at selected pressures are shown in figure 1, over the 120-180  $\text{cm}^{-1}$  range (panel a) and the 220-340  $\text{cm}^{-1}$  range (panel b). We have not carried out any attempt of

polarization analysis of the Raman signal since, as mentioned above, the sample consisted of fine crystal powder. We recall that the predicted Raman active modes, listed as a function of increasing frequency, are  $E_{2g}^2$ ,  $E_{1g}$ ,  $A_{1g}$ , and  $E_{2g}^1$ . The  $E_{2g}^2$  mode observed at about  $25\text{ cm}^{-1}$  [14] is not detectable owing to the intense low-frequency elastic and quasi-elastic scattering, as well as the  $E_{1g}$  Raman mode (at around  $170\text{ cm}^{-1}$  [14]) which can be observed only on a single crystal with a proper polarization configuration. The spectrum collected at ambient pressure with the sample already loaded in the DAC is characterized by the most intense and narrow  $A_{1g}$  mode at  $243\text{ cm}^{-1}$ . The peak shows an abrupt and remarkable broadening as the sample is compressed. On this regard we notice that the  $A_{1g}$  is the only out-of-plane vibrational mode we observe. Indeed this is the vibrational mode inherently most sensitive to volume compression since the atomic vibration takes place along the  $c$ -axis which is the *soft* lattice direction [11,15]. The  $E_{2g}^1$  mode which is detectable when the sample is on a microscope slide, actually disappears when the powder is loaded in the DAC. As the powder is compressed and pressure is applied on the sample, the  $E_{2g}^1$  appears and it becomes increasingly evident.

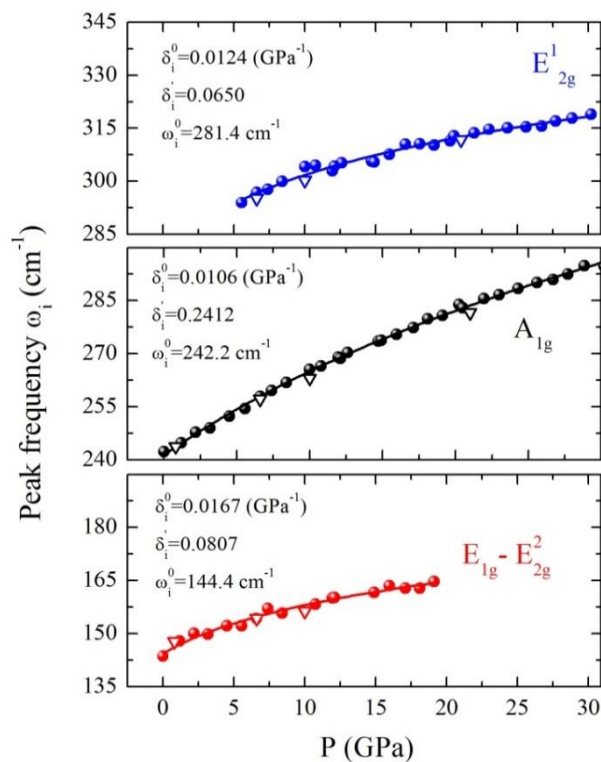


**Figure 2.** Pressure dependence of the three Raman peaks.  
Full lines: best fit curves obtained from eq. (1).

At ambient pressure, the second order Raman peak ascribed to the  $E_{1g} - E_{2g}^2$  difference mode can be found at  $143\text{ cm}^{-1}$  and it can be followed on increasing the pressure up to about 20 GPa, whereas the experimental noise masks the signal on further increasing the pressure. The weak broad peak above  $300\text{ cm}^{-1}$ , ascribed to a combination band [14], appears at ambient pressure and it is still detectable on increasing the pressure.

As expected [11,15,18], the pressure dependences shown by all the frequencies of the measured Raman peaks show a clear hardening as the sample is compressed. In order to analyze the pressure dependence of the Raman peaks, a fitting procedure has been applied to extract the central peak frequency and the linewidth. Standard Lorentz functions have been used to model the Raman signal. In the low panels in figure 1, we report an example of best-fit at 5.6 GPa. The best fit parameters

obtained for the  $A_{1g}$ ,  $E^l_{2g}$  and the  $E_{1g} - E^2_{2g}$  second-order Raman modes are shown in figure 2 (peak frequency) and figure 3 (full-width at half-maximum, FWHM) as a function of pressure. Looking at figure 2 we notice that a remarkable frequency hardening is induced by pressure and that the continuous and regular trend observed is in agreement with the previously claimed [11,15,18] absence of any structural transition within the explored pressure range. We also collected several spectra on releasing the pressure at 21, 10, 6 and 0.8 GPa. The corresponding peak frequencies (see empty triangles in figure 2) perfectly follow the behavior observed on increasing pressure with no evidences of hysteretic processes, confirming again the absence of structural transitions. A close inspection of figure 2 shows a weak sublinear pressure dependence of the mode frequencies which have then been analyzed assuming a pressure dependence given by the widely used relation [19]:

$$\omega_i(P)/\omega_i^0 = [(\delta_i^0/\delta_i')P + 1]^{\delta_i'} \quad (1)$$

where  $\omega_i^0$ ,  $\delta_i^0$ , and  $\delta_i'$ , are taken as free fitting parameters. The best fit curves are also shown in figure 2, where a very good experimental/theoretical agreement can be appreciated. The best fitting parameters are reported in figure 2. For a direct comparison we also report the slopes obtained from a simple linear fit (i.e. by setting  $\delta_i' = 1$ ) that is: 1.77 cm<sup>-1</sup>/GPa, 0.92 cm<sup>-1</sup>/GPa, 0.98 cm<sup>-1</sup>/GPa for the  $A_{1g}$ ,  $E^l_{2g}$  and the  $E_{1g} - E^2_{2g}$  modes respectively. The strong difference between the pressure sensitivity of the  $A_{1g}$  mode and the  $E^l_{2g}$  and  $E_{1g} - E^2_{2g}$  modes is explained by the larger lattice compression along the soft direction (*c*-axes) and the out-of-plane / in-plane nature of the vibrational modes. In particular the  $A_{1g}$  phonon, which involves the weak VdW forces along the *c*-axis, is more sensible to volume compression than the  $E^l_{2g}$ , which is a planar mode related to the strong covalent bond in the Se-Mo-Se planes [11,15].

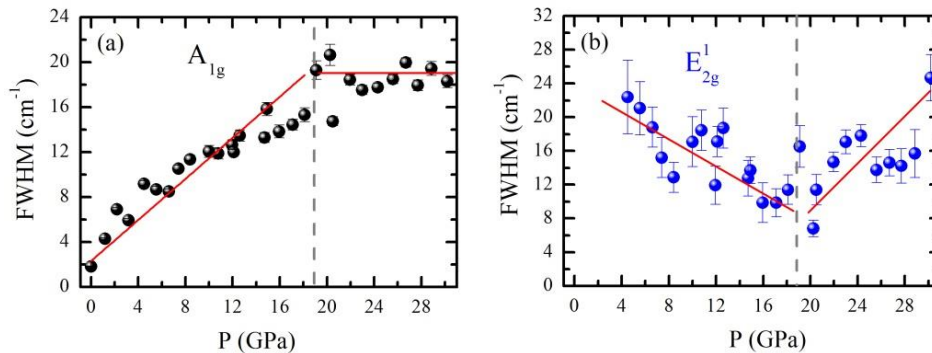


**Figure 3.** Pressure dependence of the FWHM of the  $A_{1g}$  and  $E^l_{2g}$  phonons. The vertical dashed lines and the solid red line are guide for the eye.

The full-widths at half-maximum, also obtained through the fitting procedure, are reported in figure 3 for the  $A_{1g}$  (panel a) and  $E^l_{2g}$  (panel b) peaks. A very different pressure dependence is evident, although in both cases an abrupt change occurs within the 18-20 GPa pressure range. As a function of the increasing pressure, the  $A_{1g}$  phonon shows an increasing FWHM (see panel a) up to ~19 GPa and on further increasing the pressure the linewidth keeps nearly constant. In the case of the  $E^l_{2g}$  (see panel b) a very different behavior is observed, but a turning point occurs at about the same pressure range. Bearing in mind that the high pressure infrared measurements show that a metallization process starts in the 16-20 GPa pressure range [11], the linewidth pressure behavior here observed establish a rather clear spectroscopic signature of the onset of the metallization process.

A similar anomaly has been indeed found in the pressure behavior  $\text{MoS}_2$ , where a sharp drop in the width of both the  $A_{1g}$  and the  $E^l_{2g}$  phonons was observed during the semiconducting-metal phase transition [6]. These results suggests an important role of the Raman FWHM of the  $A_{1g}$  and  $E^l_{2g}$  phonons in  $\text{MoX}_2$  TMDs materials in identifying the insurgence of a metallization process.

We want to finally mention that such a strong sensitivity of the phonon peak linewidths to electronic modifications has been previously observed in a variety of systems (e.g. in pure Te [20]) and in many high pressure studies on strongly correlated electron systems (see for example [12]). The phonon peak width is indeed directly related to charge-lattice coupling and charge transfer processes which directly monitor the electronic state and the degree of charge delocalization of the system.

### 3. Conclusion

We carried out Raman measurements on MoSe<sub>2</sub> crystal powder as function of pressure up to 30 GPa. The evolution of the frequencies of the vibrational modes  $A_{1g}$ ,  $E'_{2g}$  (Raman first order) and  $E_{1g} - E'^2_{2g}$  (Raman second-order) under applied pressure does not exhibit anomalies and can be very well reproduced by a sublinear curve. This confirms the absence of any structural transition within the 0-30 GPa pressure range, in agreement with experimental and theoretical results previously reported. More interestingly, a line-shape analysis of the Raman peaks reveals a clear anomaly in the  $A_{1g}$  and  $E'_{2g}$  linewidth pressure behavior within the pressure range 18-20 GPa. This anomaly can be ascribed to the onset of the pressure induced semiconductor-metal transition observed in previous infrared and transport experiments. Present results suggest the use of a careful line-shape analysis of the Raman spectra to detect even subtle electronic rearrangement induced by the applied pressure.

### References

- [1] Wang Q H, Kalantar-Zadeh K, Kis A, Coleman J N and Strano M S 2013 *Nature Nanotech.* **7** 699; Tang Q and Zhou Z 2013 *Progress in Materials Science* **58** 1244-1315
- [2] Wilson J and Yoffe A 1969 *Adv. Phys.* **18** 193
- [3] Tongay S, Zhou J, Ataca C, Lo K, Matthews T S, Li J, Grossman J C and Wu J 2012 *Nano Lett.* **12** 5576-5580
- [4] Capitani F, Hoepfner M, Joseph B, Malavasi L, Artioli G A, Baldassarre L, Perucchi A, Piccinini M, Lupi S, Dore P, Boeri L and Postorino P 2013 *Phys. Rev. B* **88** 144303
- [5] Bandaru N, Kumar R S, Sneed D, Tschauner O, Baker J, Antonio D, Luo S-N, Hartmann T, Zhao Y and Venkat R 2014 *J. Phys. Chem. C* **118** 3230
- [6] Nayak A P, Bhattacharyya S, Zhu J, Liu J, Wu X, Pandey T, Jin C, Singh A K, Akinwande D and Lin J F 2014 *Nat. Commun.* **5** 3731
- [7] Chi Z-H, Zhao X-M, Zhang H, Goncharov A F, Lobanov S S, Kagayama T, Sakata M and Chen X-J 2014 *Phys. Rev. Lett.* **113** 036802
- [8] Hromadová L, Martoňák R and Tosatti E 2013 *Phys. Rev. B* **87** 144105
- [9] Riflikova M, Martoňák R and Tosatti E 2014 *Phys. Rev. B* **90** 035108
- [10] Aksoy R, Selvi E and Ma Y 2008 *J. Phys. Chem. Solids* **69** 2138
- [11] Zhao Z *et al.* 2015 *Nat. Commun.* **6** 7312
- [12] Congeduti A, Postorino P, Caramagno E, Nardone M, Kumar A and Sarma D D 2001 *Phys. Rev. Lett.* **86** 1251
- [13] Bera A, Pal K, Muthu D V S, Sen S, Guptasarma P, Waghmare U V, and Sood A K 2013 *Phys. Rev. Lett.* **110** 107401
- [14] Sekine T, Izumi M, Nakashizu T, Uchinokura K and Matsuura E 1980 *J. Phys. Soc. Jpn.* **49** 1069-1077 (1980)
- [15] Bhatt S V, Deshpande M P, Sathe V, Rao R and Chaki S H 2014 *J. Raman Spectrosc.* **45** 971-979
- [16] Mao H K, Bell P M, Shaner J W and Steinberg D J 1978 *J. Appl. Phys.* **49** 3276
- [17] Capitani F, Koval S, Fittipaldi R, Caramazza S, Paris E, Mohamed W S, Lorenzana J, Nucara A, Rocco L, Vecchione A, Postorino P and Calvani P 2015 *Phys. Rev. B* **91** 214308
- [18] Sugai S and Ueda T 1982 *Phys. Rev. B* **26** 6554
- [19] Postorino P, Congeduti A, Degiorgi E, Itié J P and Munsch P 2002 *Phys. Rev. B* **65** 224102
- [20] Marini C, Chermisi D, Lavagnini M, Di Castro D, Petrillo C, Degiorgi L, Scandolo S and Postorino P 2012 *Phys. Rev. B* **86** 064103